Radar Signal Processing using Multidimensional Fast Fourier Transform

Prateek Walia, 300310026

University of Ottawa

ELG 5376 – Digital Signal Processing (Fall 2022)

Professor Martin Bouchard

Abstract

The Fast Fourier Transform (FFT) technique is frequently used to analyze signals obtained from radar sensors. This report presents a simulation design based on the multidimensional FFT algorithm to estimate the distance, relative radial velocity, and azimuth angle of arrival/departure for a target present in a two-dimensional space using synthesized frequency-modulated continuous wave (FMCW) radar signals. The simulation design includes synthesizing the FMCW radar beat signal, which is the difference between transmitted and received signals from the radar sensors. The signal processing sequence used for building this simulation includes identifying the region of interest, multidimensional FFT, peak detection, and data scaling for obtaining targets' initial radial distance, radial velocity, and azimuth angle in a two-dimensional region. The simulation results show that this method can provide high resolution in range and velocity detection with low complexity.

Keywords: Fast Fourier Transform, FFT, frequency modulated continuous wave, FMCW, radar

Table of Contents

Introduction **5**

Methodology **7**

Radial Distance Estimation 8

Radial Velocity Estimation 8

Azimuth Angle Estimation 9

Implementation **11**

Results and Discussions **22**

List of Figures

Fig. 1. Distance (in meters) vs Doppler Velocity (in km/hr). 12

Fig. 2. Fig. 2. Distance vs Doppler Velocity (zoomed at cluster 1). 12

Fig. 3. Distance vs Doppler Velocity (zoomed at cluster 2). 13

Fig. 4. Radial distance (range) plot for two targets at 100m and 200m. 15

Fig. 5. Radial Velocity plot for two targets with velocities -50 km/hr and 70 km/hr. 15

Fig. 6. Sin(azimuth) in radians vs Normalized FFT magnitude. 16

Fig. 7. Azimuth angle (in degrees) vs Normalized FFT magnitude. 17

Fig. 8. Sin(azimuth) (in radians) Distance (in meters) vs plot. 18

Fig. 9. Sin(azimuth) (in radians) Distance (in meters) vs plot (zoomed). 18

Fig. 10. Radial distance (range) plot for two targets at 100m and 200m (using Azimuth-Range). 19

Fig. 11. Azimuth angle (in degrees) for targets at -60^{o} and 45^{o} (using Azimuth-Range dimensions). 20

Fig. 12. Birds' eye view of the targets (using peak range-sin(azimuth) values). 21

Introduction

Frequency-modulated continuous wave (FMCW) radars can be dated back to the 1940s when the first FMCW radar was built for surveillance applications [1]. The moving target indication using processing FMCW radar signals was first seen in [2]. Linear FMCW radar systems have been widely employed in automotive and surveillance applications due to their low complexity and lower transmitted power compared to ultra-wideband pulse-type radar [3]. FMCW radar systems generally consist of one transmitting antenna, multiple receiving antennas, a low-noise signal amplifier (LNA), an analog-to-digital converter (ADC), a low-pass filter, and a processing unit such as a field programmable gate array (FPGA). FMCW radars use the transmitting antenna, which sends out bursts of chirps that are linearly modulated continuous waveforms with sawtooth modulation. The linearly placed patch receiver antennas receive the reflected chirp signals back, including a delay introduced by the waveform going in a round trip to each target. The received chirp signals are then passed through a low-noise amplifier that amplifies the low-powered radar signal while maintaining a high signal-to-noise ratio. The intermediate frequency process then takes place where the transmitted chirp signal frequencies are subtracted from the received chirp signal at different receiver antennas. This process results in the synthesis of a beat signal, which is an intermediate frequency signal. An analog-to-digital converter is used at the end of the chain to discretize the beat signal, a continuous waveform. The discretized wave signal is then sent to a processing device such as an FPGA or a DSP processor for implementing signal processing techniques such as the Fourier transform to extract the information of the targets present in the field of view of the radar.

This project presents the simulation design for an FMCW radar, which includes synthesis of the beat signal using a complex exponential, performing multidimensional FFT on the beat signal, peak identification, and data scaling for obtaining the initial distance, velocity, and azimuth angle of targets in a two-dimensional region.

Methodology

The Linear FMCW radar system transmits a chirp signal in the electromagnetic wave spectrum, which is linearly modulated using a modulation waveform. Different modulation waveforms, such as sawtooth modulation, sinusoidal modulation, triangular modulation, etc., can be used for different applications. This project, however, is based on chirp signals that are linearly modulated using the sawtooth waveform. This chirp signal is linearly modulated in frequency over time, so the signal begins at a low frequency but becomes a high-frequency signal after modulation over a period. The transmitted chirp signal in an FMCW radar system is given in eq. 1.

$$x(t) = \cos(2\pi(f_{carrier} + BW/T_{chirp} \times t^2/2)) \tag{1}$$

The receiver antennas then receive a signal back reflected from the target, which is just a time-shifted transmitted signal with the delay caused due to the round trip of the signal. The received signal at each receiver antenna can be expressed as in eq. 2.

$$x(t-t') = cos(2\pi\frac{2 * fcarrier(d + v(l-1)T_{chirp)}}{c} + \frac{2BWd}{T_{chirp}c}t + \frac{d_s(k-1)\sin(\theta_m)}{\lambda_c arrier}) \tag{2}$$

$$0 < t < T_{chirp}, 1 \leq l \leq N_{chirp}, 1 \leq k \leq N_{antennas}$$

From [4], if more N number of targets are present, the received signal will be a sum of individual received signals. Therefore, if m targets are present, the received continuous-time waveform, and if echo is neglected, the received signal is given by eq. 3.

$$x(t-t') = \sum_{m=1}^{N_{targets}} cos(2\pi\frac{2 * fcarrier(d + v(l-1)T_{chirp)}}{c} + \frac{2BWd}{T_{chirp}c}t + \frac{d_s(k-1)\sin(\theta_m)}{\lambda_c arrier}) \tag{3}$$

$$0 < t < T_{chirp}, 1 \leq l \leq N_{chirp}, 1 \leq k \leq N_{antennas}$$

We can see that if an object is close to the radar, the time difference t` will be small, and as the object moves farther away, the time difference t` will keep increasing. Thus, a relation between t` and the object's distance can be used to measure the target's distance from the radar. The beat signal generated in the IF step of the radar process is discretized using an ADC the resulting eq. 4 is obtained.

$$y_{l,k}[n] = \cos(2\pi(2\frac{BWd_m}{T_{chirp}c}nT_s + 2\frac{v_m}{\lambda_{carrier}}(l-1)T_{chirp} + \frac{d_s\sin(\theta_m)}{\lambda_{carrier}}(k-1)) \tag{4}$$

$$0 \leq n \leq \lfloor T_{chirp}/T_s \rfloor - 1, 1 \leq l \leq N_{chirp}, 1 \leq k \leq N_{antennas}$$

Radial Distance Estimation

If we were to perform an FFT, we would observe a peak corresponding to the distance of a target at a particular sample which can then be used to estimate the range and be scaled to appropriate units. Such peaks corresponding to each target distance will be observed if multiple targets are present. The range resolution depends on how closely present intermediate frequencies can be separated after performing the FFT. The resolution for the range is characterized in eq.5 [4].

$$D_{res} = c/(2 * BW_{chirp}) \tag{5}$$

The discrete time-frequency component in eq. 6 is used to obtain the scaling factor for estimating the distance of the targets.

$$2\frac{BWd_m}{T_{chirp}c}T_s \tag{6}$$

Radial Velocity Estimation

In the case of a moving target, the signal received by the receiver will be affected by the process known as the doppler shift. This doppler frequency shift can be observed over several chirp signals

received, which will have a constant phase shift. If FFT is applied across the chirps in the same bin where the object's distance was found, then the peak can help us find the object's velocity. Therefore, the operation for range and doppler velocity can be combined by performing a two-dimensional FFT, one FFT across the num of samples in each chirp signal and another FFT across the chirp signals. The peak in the two-dimensional FFT data can then be used to find the range and velocity information of the moving target. The discrete frequency component in eq. 7 is used to obtain the scaling factor for estimating the radial velocity of the targets.

$$2\frac{v_m}{\lambda_{carrier}}T_{chirp} \tag{7}$$

For the velocity resolution the constraint is on identifying the phase shift using different chirp signals. Eq. 8 is used to find the velocity resolution [5].

$$V_{res} = \lambda_{carrier}/(2 * numberchirps * T_{chirp}) \tag{8}$$

Azimuth Angle Estimation

To also estimate the angle of arrival or departure of the targets, multiple receiving antennas are used and the discrete frequency component in eq. 9 is used to find the appropriate scaling factor for the azimuth angle.

$$\frac{d_s \sin(\theta_m)}{\lambda_{carrier}} \tag{9}$$

To find the azimuth angle two methods can be used where a three-dimensional FFT can be performed across the number of chirp signals, number of samples per chirp, number of antennas. The corresponding peaks in this 3D FFT data will then give us the arrange, velocity, and angle information of the targets. However, this is computationally expensive and is not required. Instead,

the peak identified for the initial 2D FFT can be used and a 3rd 1D-FFT performed only at the location where the range-velocity information is detected. The resulting FFT will provide us with the angle of the target after scaling using eq. 9.

Implementation

Initially, the target parameters are defined to simulate the presence of targets in the two-dimensional space. The test case used is:

- Target 1 at a radial distance of 100 meters, a relative radial velocity of -50 km/hr, and an azimuth angle of -60 degrees.
- Target 2 at a radial distance of 200 meters, a relative radial velocity of 75 km/hr, and an azimuth angle of 45 degrees.

Then, the radar parameters, such as desired maximum range and range resolution, maximum velocity and velocity resolution, and the number of antennas present in the design, are defined. Based on this, user-defined parameters chirp signal parameters are computed. The total signal time or the observation time is 34.456 ms, as mentioned in [4]. The number of samples in each signal and the number of chirps is calculated using eq. 10 and eq 11.

$$number\ of\ samples = 2 * (\frac{max\ distance}{distance\ resolution}) \tag{10}$$

$$number\ of\ chirps = 2 * (\frac{max\ velocity}{velocity\ resolution}) \tag{11}$$

For these parameters, the next power of two was chosen for faster FFT computation. The sampling frequency was 2.5 times the maximum frequency present in the beat signal to meet the Nyquist rate. After defining the parameters required for the beat signal, beat signal synthesis is performed. Three nested for loops are used, and a three-dimensional data cube is formed with a row equal to the number of samples in each chirp signal, columns equal to the number of chirp signals, and third-dimension tubes equal to the number of receiver antennas in the radar.

After the 3-dimensional data cube was created, a two-dimensional FFT was computed using the MATLAB function *fft2,* along with the number of chirps and samples in each chirp. This two-dimensional data of size number of chirps x number of samples in each chirp was used two compute the magnitude of the two-dimensional FFT. The magnitude response of the FFT was centered at zero using the MATLAB function *fftshift.* Using an appropriately scaled axis, a two-dimensional plot was created using the function *imagesc* for the distance-doppler velocity information. In the plot (Fig. 1), the peaks detected correspond to the targets present in the two-dimensional space.

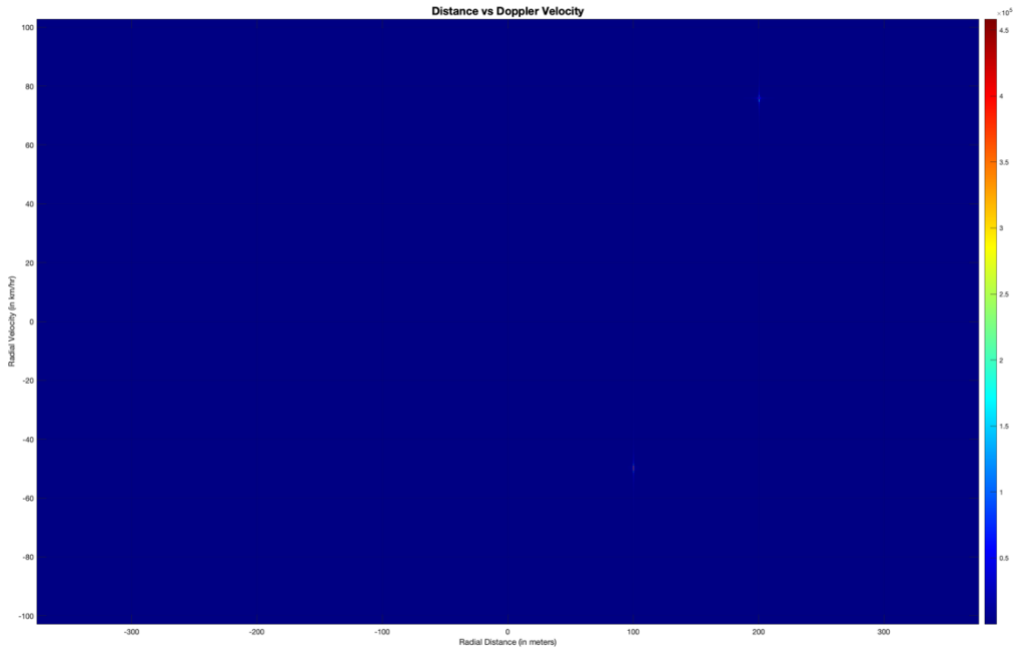

Fig. 1. Distance (in meters) vs Doppler Velocity (in km/hr).

If zooms are performed on the clusters with higher magnitudes Fig. 2 and Fig. 3, the user-defined parameters of distance and velocity of the targets can be verified.

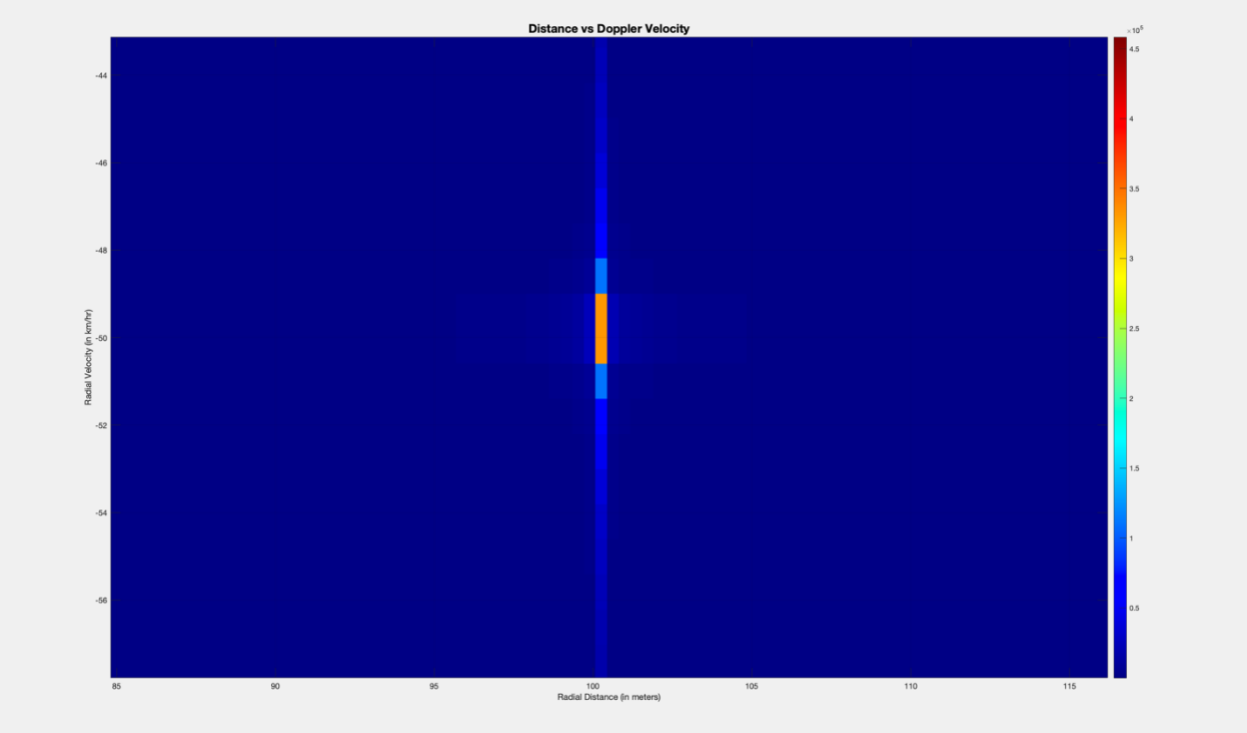

Fig. 2. Distance vs Doppler Velocity (zoomed at cluster 1).

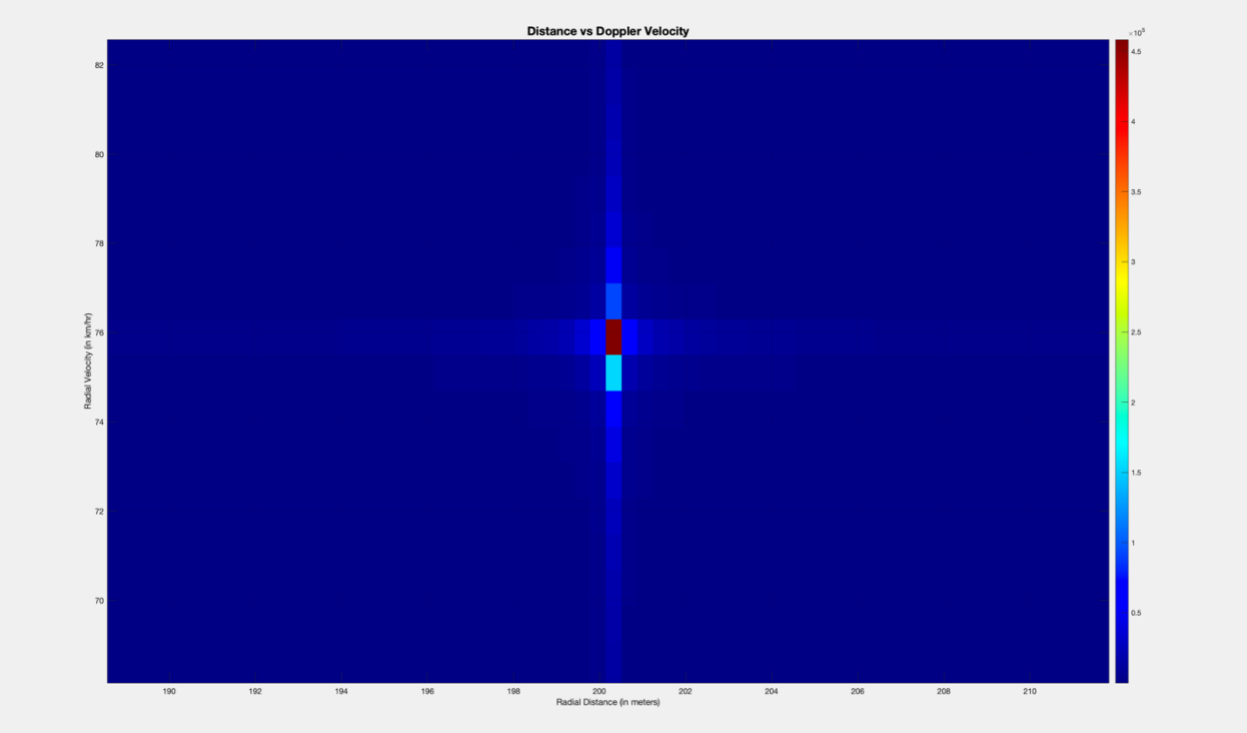

Fig. 3. Distance vs Doppler Velocity (zoomed at cluster 2).

After creating a two-dimensional data plot to improve the visibility of the distance and velocity information of the targets', plots using the horizontal and vertical direction of the two-dimensional FFT magnitude data matrix were created A first maximum value was found using two nested for loops, and the indices of the maximum values were located using *the find* method. For finding the second maximum again, two nested for loops were used. However, additional conditions that defined the minimum distance between the rows and columns from the first maximum were added. This was done to ensure that the two maximum values were not picked up from the same cluster representing a single target. Initially, this condition was missing, resulting in missing one out of the targets for some distance and velocity test cases. The rows and columns to be plotted were identified based on the two maximum values in the two-dimensional FFT magnitude matrix. In Fig. 4 and Fig. 5, it can be observed that it is considerably easier to view the distance and velocity information of the two targets accurately. To enhance the visibility of the results, the FFT magnitude was normalized, thus giving two easily distinguishable peaks. The negative distances have not been excluded in this simulation to indicate if the target is present behind the radar. Also, negative velocities indicate whether the target is incoming or outgoing, where negative velocity indicating that target is incoming and positive velocity indicating that target is outgoing.

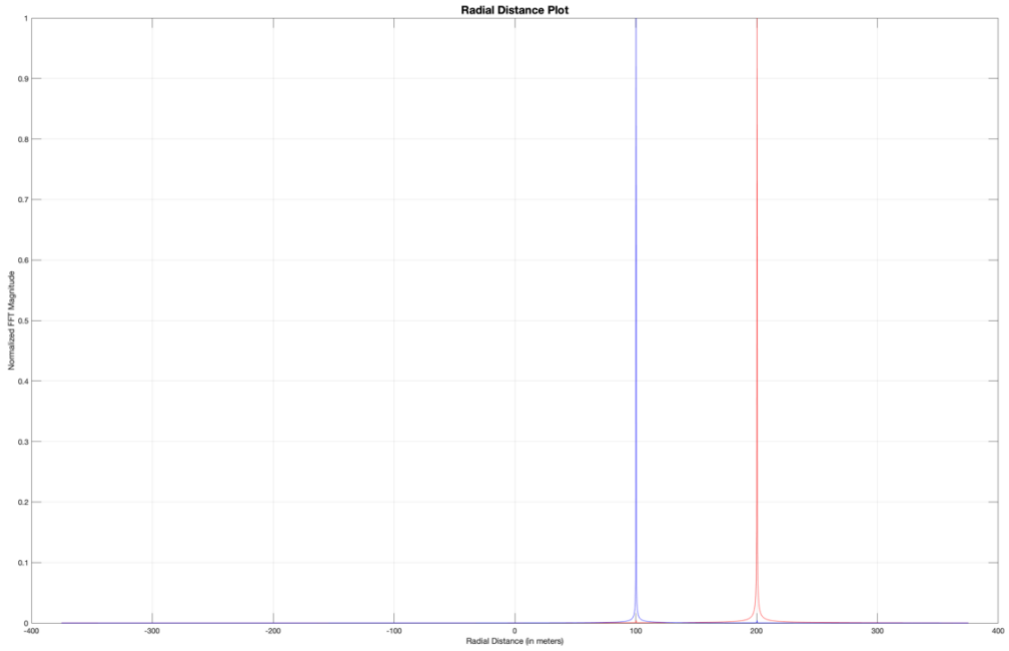

Fig. 4. Radial distance (range) plot for two targets at 100m and 200m.

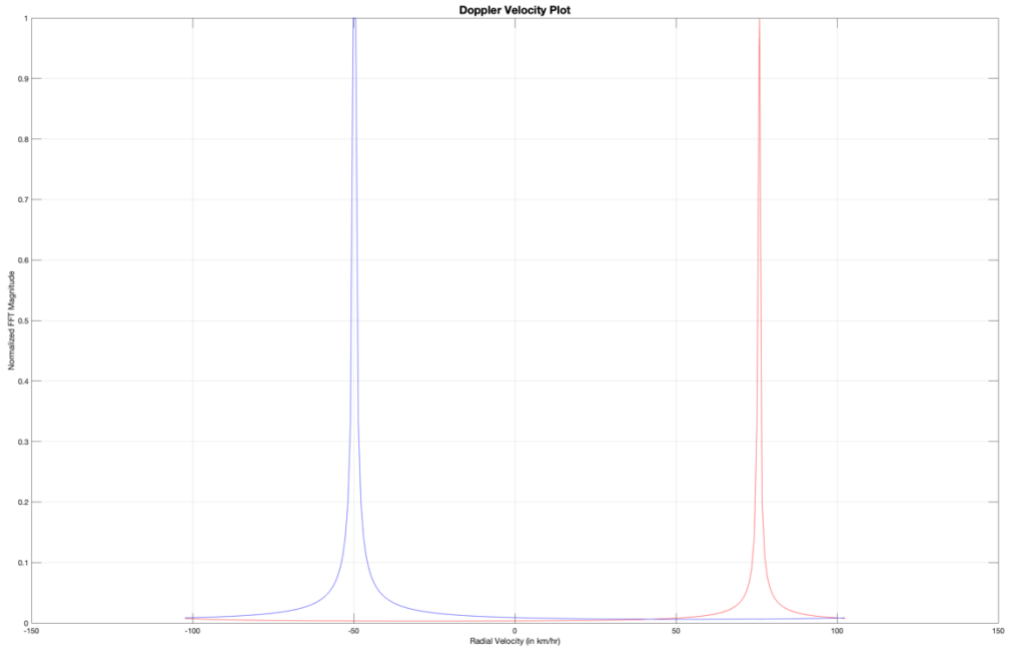

Fig. 5. Radial Velocity plot for two targets with velocities -50 km/hr and 70 km/hr.

After this, a three-dimension FFT was performed for the original beat signal data cube with the number of chirps, samples, and antennas x 32. The times 32 factor for the number of antennas was introduced to perform zero padding in the third dimension of the beat signal matrix for better computation resolution in the frequency response. After the computation of the three-dimensional FFT, a new 3D data cube was created with the shifted magnitude values of the three-dimensional FFT. In this three-dimensional FFT, the location of the identified peaks from the distance-velocity 2D FFT was used as the peak values would identify the region of interest for the targets, and the 3D FFT was plotted for max row and max column across the azimuth dimension. This results in a sin(azimuth) angle plot (Fig. 6). The x-axis, by default, was plotted in radians which were scaled by taking the inverse sine function using *asind*, and another Azimuth versus FFT magnitude plot was plotted (Fig. 7). Again, the FFT magnitude was normalized to identify the peaks better, and the observations were verified with the user-defined parameters of target azimuth angles.

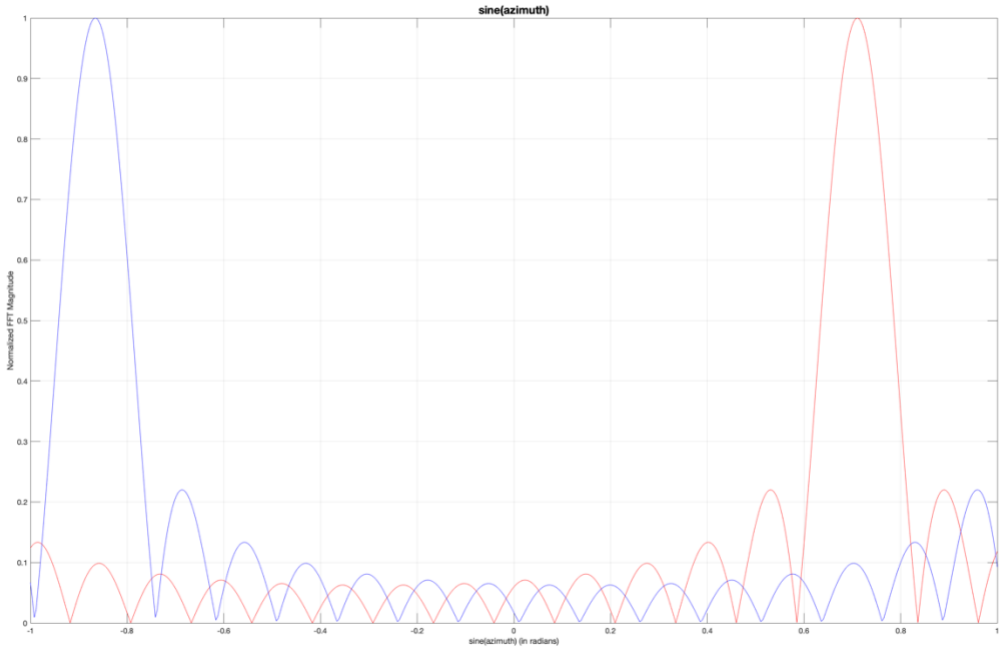

Fig. 6. Sin(azimuth) in radians vs Normalized FFT magnitude.

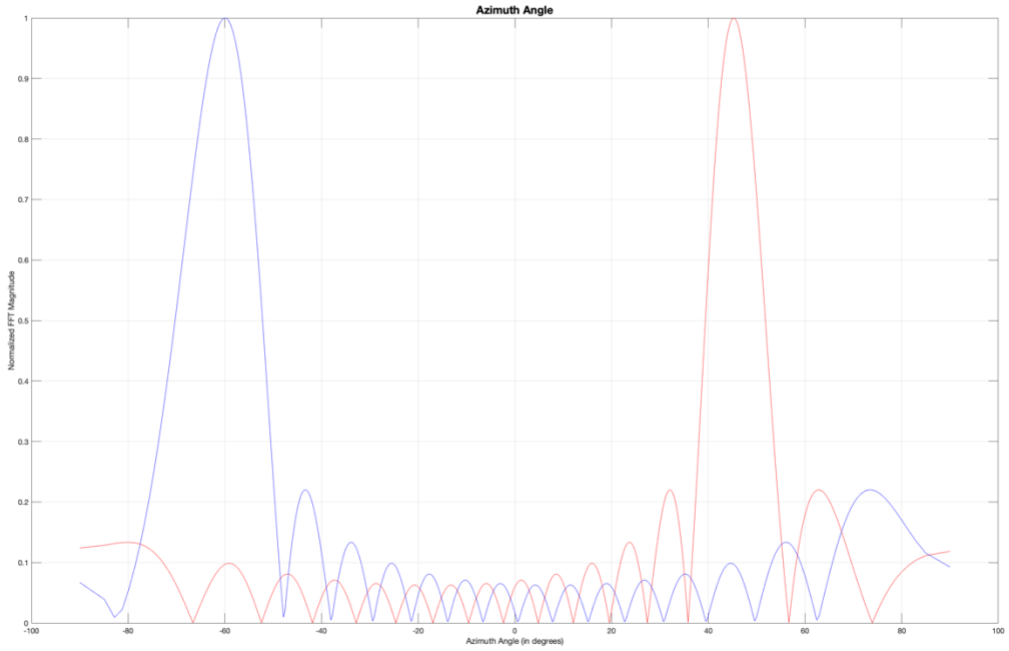

Fig. 7. Azimuth angle (in degrees) vs Normalized FFT magnitude.

Furthermore, the simulation then, instead of using the velocity dimension, relies on the distance and azimuth dimensions to estimate the distance and azimuth angle information. This is done in the case the velocity information of the target is not required. Firstly, as the velocity information is not required, any of the n_{th} numbers of chirps can be selected for finding the range and azimuth information. In this case, the first chirp signal was selected. Like the sequence mentioned above in distance-doppler velocity calculation, all the steps are repeated for the distance-azimuth information. Again, for better computational resolution, zero padding was performed by a factor of 8 in the distance dimension and 32 in the azimuth dimension. First, a 2D plot was created with the azimuth information on the x-axis the radial distance information on the y-axis (Fig. 8). In Fig.9, zoom was performed on the two cluster targets.

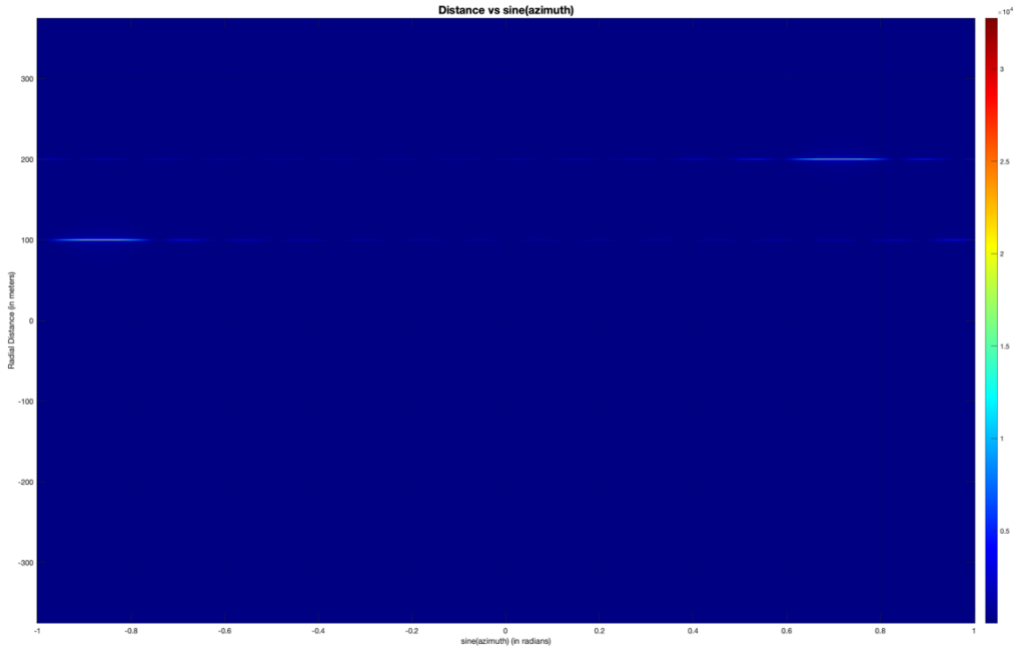

Fig. 8. Sin(azimuth) (in radians) Distance (in meters) vs plot.

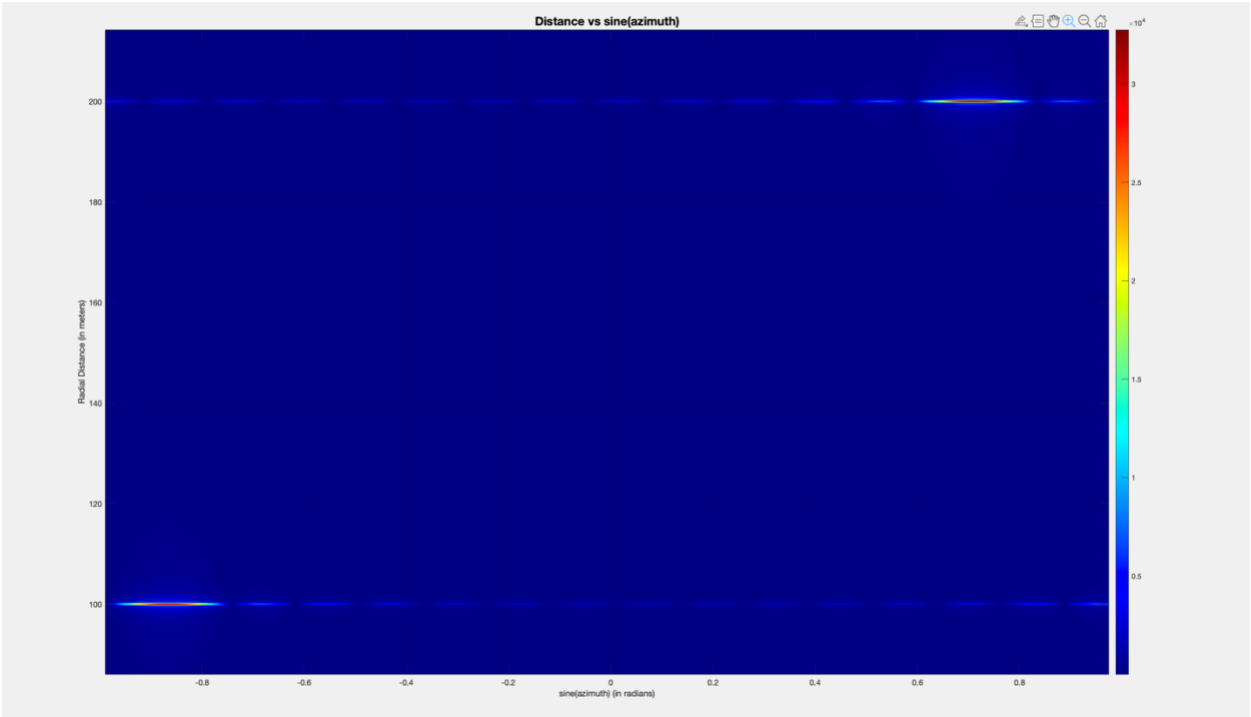

Fig. 9. Sin(azimuth) (in radians) Distance (in meters) vs plot (zoomed).

Again, the same nested for-loop method was used to identify the first and second maximum values from the two-dimension azimuth-distance FFT matrix and used to plot individual slices in horizontal and vertical directions to visualize the radial distance and azimuth angle better. The FFT magnitude was normalized and plotted against the scaled axis for azimuth and distance information. The two plots below are created (Fig. 10 and Fig. 11), and the angle and range information are verified. More ripple is seen in these plots due to zero padding before performing the FFT; however, better computational resolution of the FFT allows for easier visualization o the peaks. The distance and angles were verified based on the user-defined parameters.

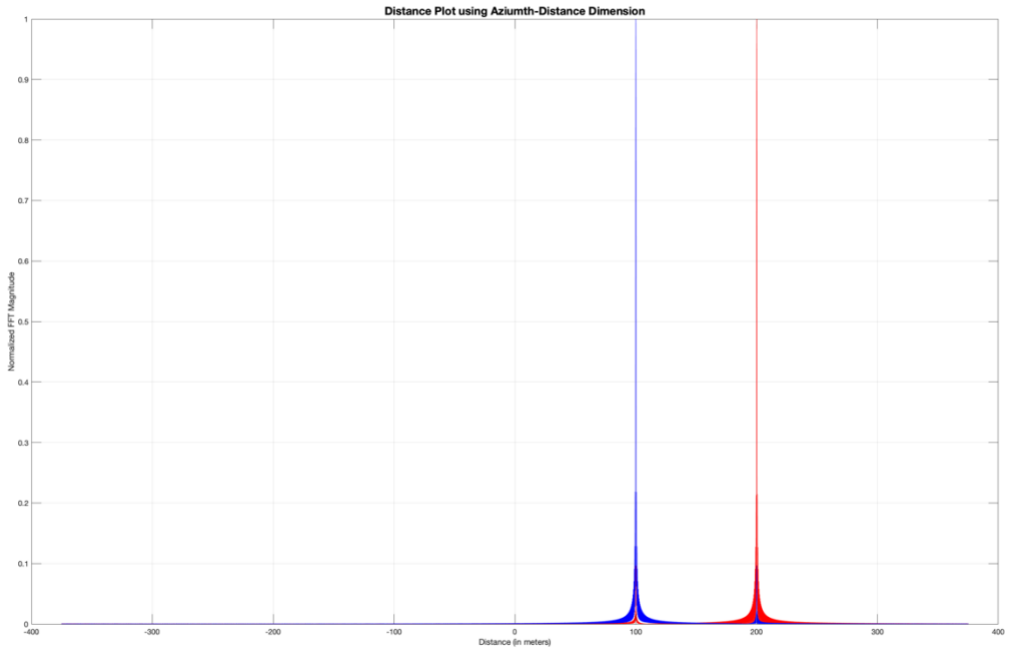

Fig. 10. Radial distance (range) plot for two targets at 100m and 200m (using Azimuth-Range dimensions).

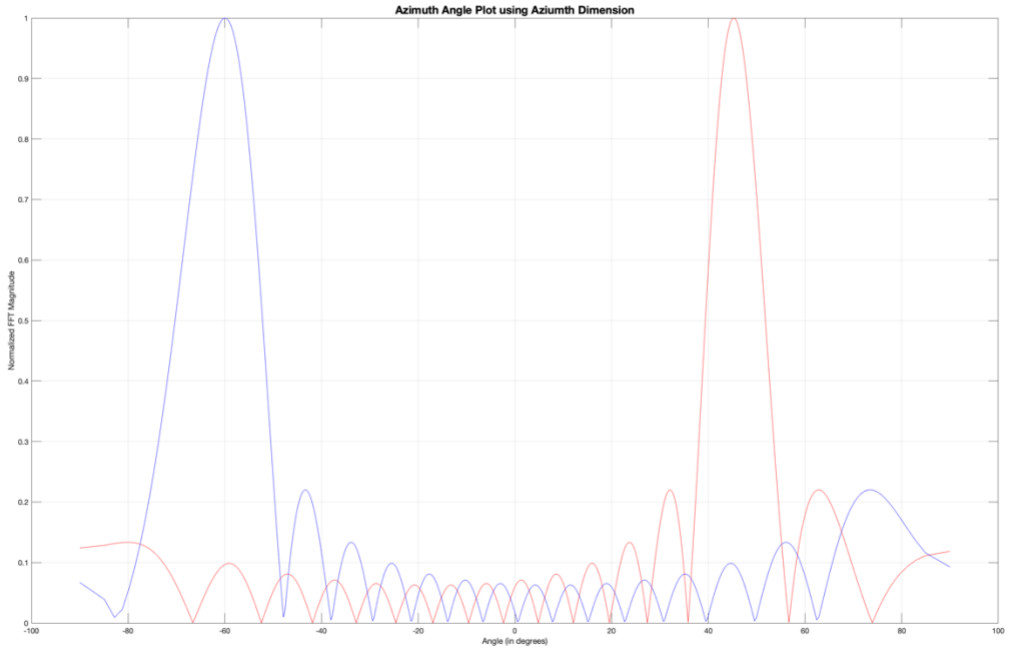

Fig. 11. Azimuth angle (in degrees) for targets at -60^{o} and 45^{o} (using Azimuth-Range dimensions).

Furthermore, a bird's eye view visualization (Fig. 12) was created to see the target locations when observed from the sky. For this plot, the lateral and ahead distances were calculated using the estimated distance and azimuth angle values for the two detected targets. For the lateral direction, the estimated distance was multiplied by the sine of the estimated azimuth angle. For the front direction, the estimated distance of the target was multiplied by the cosine of the estimated azimuth angle of the target. Following this, the cartesian plot for birds' eyes was created. Finally, the initial distance, radial velocity, and azimuth angle information were obtained by locating the peak values and then scaling the frequency samples using appropriating scaling parameters. The detected target information was displayed in the command window.

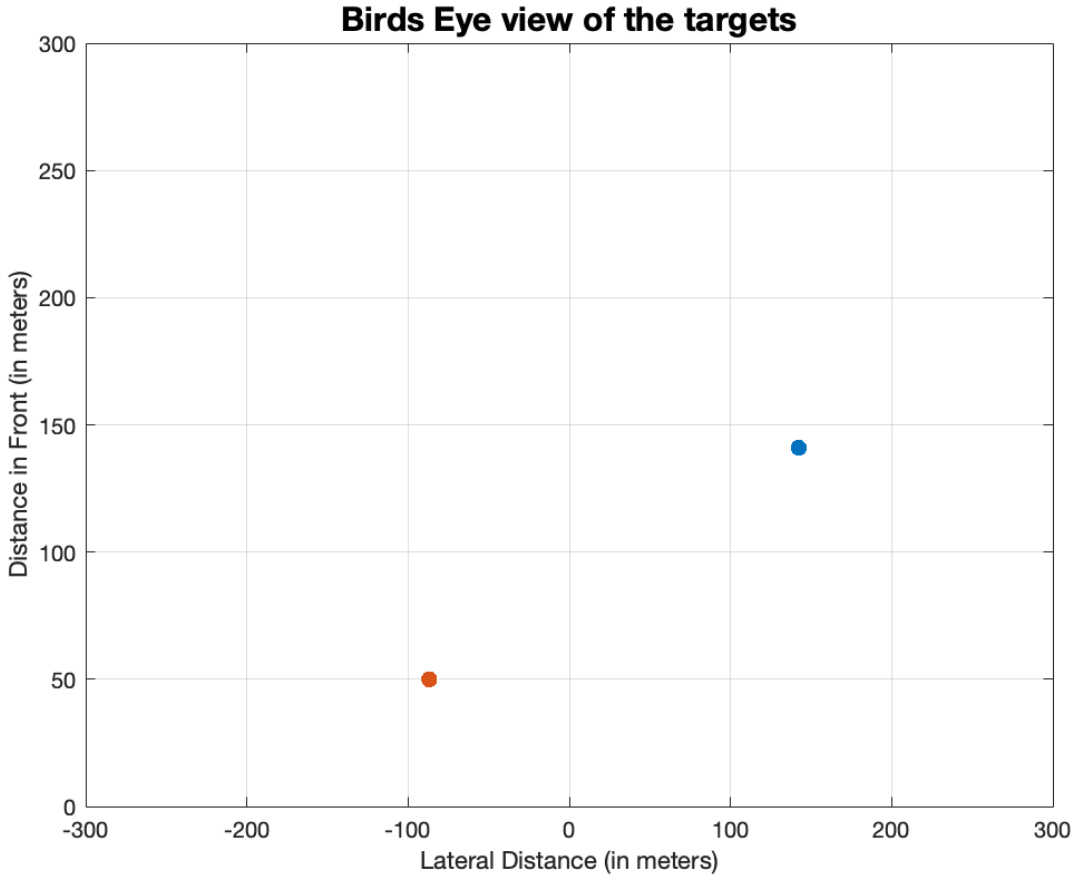

Fig. 12. Birds' eye view of the targets (using peak range-sin(azimuth) values).

Results and Discussion

The complex exponential ($e^{j\theta}$) was used to synthesize the beat signal. It was observed that in [5], the beat signal was generated using cosine, which resulted in a mirror image of each target at a negative radial distance due to the negative frequencies and required removing the negative frequencies. However, in this design the exponential form was used; and no such removal of half-frequencies is required.

Additionally, the range max and range resolution parameters, defined as 300 meters and 0.30 cm (for automotive applications) in this simulation, can be varied to match the requirements. Also, the distance was not assumed to be only positive values, and negative distances can also be observed, indicating that the target is behind the radar. The required samples can be calculated using these values to meet these criteria. To meet the parameters mentioned above, used in the test case, the number of samples in each chirp required was 2000. However, for faster FFT computation, the 2048-point DFT was chosen, the next power of 2. Increase in the value of N to 2048 was noted to produce an increase of maximum range that can be detected correctly was identified to be 307.2 meters. The simulation design was able to identify targets that were located 30 cm apart; however, the velocity information for one target was masked when the targets were located within 30 cm of each other. The lowest magnitude of distance that could be correctly identified (within Δ 30 cm) was 30 cm where the velocities were also correctly detected for the targets.

The maximum velocity and the velocity resolution values chosen were 100 km/hr and 0.8 km/hr (for automotive applications). The number of chirps required to meet these criteria was calculated

using these values. The velocity can also be negative, indicating an incoming object; therefore, the minimum velocity was taken as negative of the maximum velocity. To meet the criteria mentioned above, the number of chirps calculated was 250. However, for faster FFT computation, the 256-point DFT was chosen, which is the next power of 2. As the value of "N" was increased a subsequent increase maximum velocity range was also seen with the maximum velocity that can be detected correctly being 102.4 km/hr and the minimum velocity being -102.4 km/hr. The resolution for velocities was measured as 0.9 km/hr with the design being able to identify targets correctly with a difference of at least 0.9 km/hr in their speed.

For the maximum angle 90 degrees was chosen. In [4], the distance between antennas was the wavelength of the carrier signal, and the maximum angle for their application was 30 degrees. However, if the distance between the antennas is half of the wavelength of the carrier signal, the maximum angles that can be detected are 90 degrees in the positive and negative directions. Number of antennas used for the simulation were 16, which produced better angle resolution than the 4.1degree angle resolution obtained in [4]. The simulation design was able to obtain an angle resolution of approximately 2 degrees. The maximum and minimum angles that were identified accurately (within $\Delta 2$ degrees) was 83.5 degree and -83.5 degrees, with angles greater in magnitude than these values resulting in the azimuth angle being detected at 90 degrees. This can be resolved by increasing the number of antennas to 32, however; this would result in an increase in the computational complexity of the design.

References

[1] Stove, A. (1992). Linear FMCW radar techniques. *IEE Proceedings F Radar and Signal Processing, 139*(5), 343. doi:10.1049/ip-f-2.1992.0048

[2] D. E. Barrick, "FM/CW Radar Signals and Digital Processing", *NOAA Technical Report ERL 283-WPL 26*, 1973.

[3] Kim, B., Jin, Y., Lee, J., & Kim, S. (2022). FMCW radar estimation algorithm with high resolution and low complexity based on reduced search area. *Sensors, 22*(3), 1202. doi:10.3390/s22031202

[4] Saponara, S., & Neri, B. (2017). Radar sensor signal acquisition and multidimensional FFT processing for surveillance applications in Transport Systems. *IEEE Transactions on Instrumentation and Measurement, 66*(4), 604-615. doi:10.1109/tim.2016.2640518

[5] Stephan, M., Stadelmayer, T., Santra, A., Fischer, G., Weigel, R., & Lurz, F. (2021). Radar Image Reconstruction from raw ADC data using parametric variational Autoencoder with domain adaptation. *2020 25th International Conference on Pattern Recognition (ICPR)*. doi:10.1109/icpr48806.2021.9412858